Article

Potent Inhibitors of Subgenomic Hepatitis C Virus RNA Replication through Optimization of Indole-*N*-Acetamide Allosteric Inhibitors of the Viral NS5B Polymerase

Steven Harper, Salvatore Avolio, Barbara Pacini, Marcello Di Filippo, Sergio Altamura, Licia Tomei, Giacomo Paonessa, Di Marco, Andrea Carfi, Claudio Giuliano, Julio Padron, Fabio Bonelli, Giovanni Migliaccio, Raffaele De Francesco, Ralph Laufer, Michael Rowley, and Frank Narjes

More About This Article

Additional resources and features associated with this article are available within the HTML version:

- Supporting Information
- Links to the 5 articles that cite this article, as of the time of this article download
- Access to high resolution figures
- Links to articles and content related to this article
- Copyright permission to reproduce figures and/or text from this article

View the Full Text HTML

Potent Inhibitors of Subgenomic Hepatitis C Virus RNA Replication through Optimization of Indole-*N*-Acetamide Allosteric Inhibitors of the Viral NS5B Polymerase

Steven Harper,* Salvatore Avolio, Barbara Pacini, Marcello Di Filippo, Sergio Altamura, Licia Tomei, Giacomo Paonessa, Stefania Di Marco, Andrea Carfi, Claudio Giuliano, Julio Padron, Fabio Bonelli, Giovanni Migliaccio, Raffaele De Francesco, Ralph Laufer, Michael Rowley, and Frank Narjes

IRBM (Merck Research Laboratories, Rome), Via Pontina km 30,600, 00040 Pomezia, Rome, Italy

Infections caused by hepatitis C virus (HCV) are a significant world health problem for which novel therapies are in urgent demand. Compounds that block replication of subgenomic HCV RNA in liver cells are of interest because of their demonstrated antiviral effect in the clinic. In followup to our recent report that indole-*N*-acetamides (e.g., **1**) are potent allosteric inhibitors of the HCV NS5B polymerase enzyme, we describe here their optimization as cell-based inhibitors. The crystal structure of **1** bound to NS5B was a guide in the design of a two-dimensional compound array that highlighted that formally zwitterionic inhibitors have strong intracellular potency and that pregnane X receptor (PXR) activation (an undesired off-target activity) is linked to a structural feature of the inhibitor. Optimized analogues devoid of PXR activation (e.g., **55**, EC_{50} = 127 nM) retain strong cell-based efficacy under high serum conditions and show acceptable pharmacokinetics parameters in rat and dog.

Introduction

Despite well over a decade having passed since hepatitis C virus (HCV) was identified as the pathogen responsible for most cases of non-A and non-B hepatitis,[1] HCV infection continues to pose a significant world health problem.[2] There are around 170 million carriers of the virus worldwide, and increasingly, members of this community are facing medical complications that result from disease progression. HCV can lead to life-threatening liver disorders such as cirrhosis and hepatocellular carcinoma and is now recognized as the single leading cause of liver transplantation.[3] The gravity of HCV infection is compounded by the inadequacy of currently approved treatments for the disease. These are based on modified interferons that are expensive, poorly tolerated, and show variable success rates.[4]

While new therapies to tackle HCV are urgently needed, efforts toward them have been impeded by the complex biology associated with the virus. HCV is not infectious in cell culture or in small animal models, presenting a significant challenge to the development of anti-HCV agents. However, the recent introduction of the HCV replicon assay,[5] a surrogate cell-based system in which replication of subgenomic viral RNA can be studied, has provided a crucial advance for drug discovery efforts targeting HCV proteins. This assay is validated by the observation that an inhibitor of a viral enzyme, the NS3 protease,[6] shows potency in this system and also elicits a strong reduction in viral titer in a clinical setting.[7] Consequently the search for compounds that efficiently block HCV replication in the replicon assay has become an intense area of pharmaceutical research.

In addition to NS3, the nonstructural region of the HCV genome encodes several additional enzymes that are believed to play fundamental roles in the viral life cycle and that are viable targets for drug discovery efforts. The NS5B protein is one of these and has been characterized as the RNA polymerase enzyme that catalyzes the synthesis of both a complementary (−)-stranded HCV RNA intermediate and the (+)-stranded viral genome itself.[8] In common with other nucleotide polymerizing enzymes, NS5B adopts a tertiary structure that resembles a right hand, with three constitutive peptide domains designating the palm, fingers, and thumb.[9] The catalytic action of the enzyme is mediated by two magnesium ions that are ligated in the palm domain and serve to activate the 3′-OH of the elongating RNA and to position the incoming nucleotide triphosphate for nucleophilic attack.

NS5B has emerged as an especially attractive target for drug discovery efforts toward antivirals for HCV and has been described as the most drugable HCV protein.[10] The absence of a functional counterpart to NS5B in mammalian cells, where DNA is usually the template during RNA transcription, may favor the development of selective and nontoxic inhibitors. Toward this goal several series of NS5B inhibitors that show activity in the replicon assay have been reported. Chain-terminating nucleoside analogues that bind at the active site of NS5B have been found to show potency in the submicromolar range.[11] To date, no non-nucleoside inhibitors that both bind at the active site of NS5B and show cell-based activity have been reported. However, allosteric inhibition by small-molecule inhibitors of NS5B has emerged as a bona fide route toward inhibition of subgenomic HCV RNA replication, and a number of structurally diverse inhibitor classes have now been identified.[12−14] We recently reported a series of allosteric

---

* To whom correspondence should be addressed. Phone: +39 06 91093444. Fax: +39 06 91093564. E-mail: steven_harper@merck.com.

indole-*N*-acetamide inhibitors, typified by **1**, that are potent inhibitors of the NS5B enzyme and show promising activity in the replicon assay.[15]

1

IC$_{50}$ 26 nM
EC$_{50}$ 0.8 μM
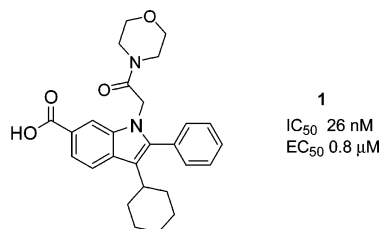
Biochemical studies[15,16] suggest that compounds of this type inhibit NS5B through interaction at a site in the thumb domain, close to proline 495. Our preliminary studies in this area revealed that inhibitors such as **1** show an encouraging overall profile, with good to excellent pharmacokinetics in rat and dog, and no significant off-target activities. In this paper we provide an account of our efforts to further optimize this series toward compounds that show improved cell-based potency and a suitable overall profile for further development as anti-HCV agents. This work was in part guided by structural information that confirmed the allosteric mechanism of action of this inhibitor class and that also played a role in guiding our SAR explorations.

Biology

The compounds described were assessed for activity against the purified ΔC$_{55}$ NS5B enzyme (IC$_{50}$) in the presence of heterogenic template RNA.[15] Inhibition of replication of subgenomic HCV RNA was measured in HUH-7 cells using a modification of the procedure of Bartenschlager.[5,15] Unless otherwise stated, cell-based data (EC$_{50}$) were measured in the presence of 10% fetal calf serum. Alternatively, this assay was run under high-serum conditions in the presence of 50% normal human serum (NHS). Pharmacokinetic parameters were determined in Sprague-Dawley rats and beagle dogs. Plasma concentrations were determined by HPLC–MS/MS analysis, and pharmacokinetic parameters were calculated by noncompartmental analysis. Activation of the pregnane X receptor (PXR) was determined[17] using HepG2 cells cotransfected with a plasmid vector encoding human PXR and a vector encoding secreted alkaline phosphatase (SEAP) under the control of a synthetic PXR-responsive DNA element. Cells were incubated for 48 h with and without test compounds, and SEAP activity was determined using a commercial detection kit.

Chemistry

Most compounds described herein were accessed from methyl 2-bromo-3-cyclohexylindole-6-carboxylate **60** as has previously been described.[15] Functionality at the 2-position of the indole was introduced via palladium-catalyzed cross-coupling chemistry, performed either prior to or after installation of the acetamide group at N1. Compounds **2**−**37** were prepared in parallel (as part of a larger array) from the appropriate C2-functionalized indole-*N*-acetic acid (**58**) utilizing the amide coupling/deprotection sequence outlined in Scheme 1. The use of polymer-bound reagent and scavenger resins during formation of the amide bond facilitated workup through simple filtration, and the carboxylic acid functionality
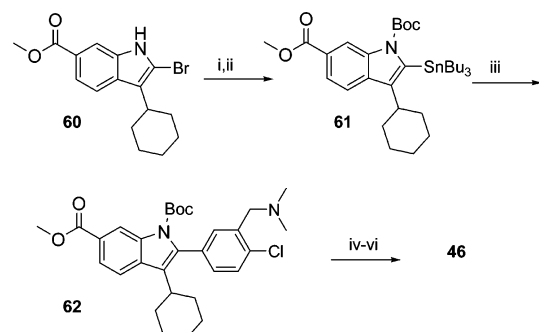
Scheme 1[a]
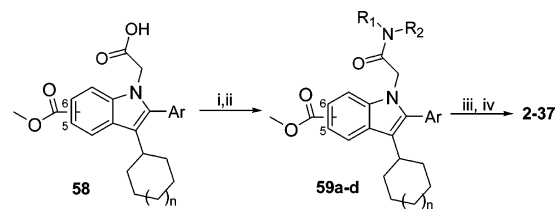
58a 6-CO$_2$H, n = 1, Ar = Ph,
58b 6-CO$_2$H, n = 1, Ar = 4-Cl-Ph
58c 5-CO$_2$H, n = 1, Ar = Ph
58d 6-CO$_2$H, n = 0, Ar = Ph

[a] Reagents and conditions: (i) PS-EDC, R$_1$R$_2$NH, CH$_2$Cl$_2$; (ii) PS-NCO; (iii) BBr$_3$, CH$_2$Cl$_2$; (iv) RP-HPLC or Isolute C$_{18}$ SPE purification.

Scheme 2[a]

[a] Reagents and conditions: (i) Boc$_2$O, DMAP, CH$_2$Cl$_2$; (ii) ^{n}BuLi, Bu$_3$SnCl, THF, −78 °C; (iii) (5-bromo-2-chlorobenzyl)dimethylamine, Pd$_2$(dba)$_3$, P^{t}Bu$_3$, dioxane, 100 °C; (iv) TFA, CH$_2$Cl$_2$; (v) NaH, ClCH$_2$CONMe$_2$, DMF; (vi) BBr$_3$, CH$_2$Cl$_2$.

was conveniently unmasked by direct addition of BBr$_3$ to the filtrate. Purification by either automated or manual RP-HPLC or by reversed-phase solid-phase extraction afforded the inhibitors in high purity (>95%) and acceptable chemical yield (about 20−40%). Compounds **40**−**43** and **49**−**57** were accessed through analogous chemistry that was performed in solution phase using HATU as the amide coupling reagent and using KOH in the subsequent deprotection step. Compounds **38** and **39** were available through a routine hydrogenation step during the synthesis of the corresponding unsaturated analogues (**40** and **41**, respectively). The aminomethyl functionality on the C2 phenyl ring of **44**, **45**, **47**, and **48** was introduced by reductive amination after Suzuki cross-coupling between **60** and the appropriate formylboronic acid.

Compound **46** was prepared as outlined in Scheme 2. The 2-stannylindole **61** was obtained through Boc protection of **60**, followed by lithium−halogen exchange and then trapping of the organolithium intermediate with tributyltin chloride. Stille cross-coupling of **61** with (5-bromo-2-chlorobenzyl)dimethylamine afforded **62**, and installation of the acetamide functionality/deprotection completed the synthesis.

Results and Discussion

In previous work that led to the identification of **1**, the role of structure−activity relationships at the C2 and N1 positions of the indole was crucial. It was found that introduction of highly lipophilic functionality on the C2 aromatic ring could provide substantial gains in enzyme affinity but had a variable effect on cell-based
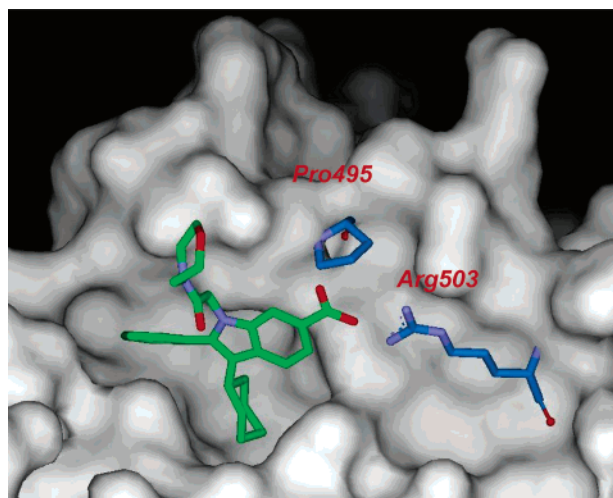
Figure 1. Enzyme-bound crystal structure of **1** at its allosteric site obtained following soaking of the inhibitor into preformed crystals of ΔC_{55} HCV NS5B. The following color scheme is used: green, carbon (inhibitor); red, oxygen; light-blue, nitrogen; dark-blue, carbon (protein); white, space-filling representation of solvent-exposed protein surface.

activity. In contrast, the structure of substituents on the indole nitrogen atom had little influence on intrinsic potency but was fundamental in dictating cell-based efficacy, suggesting that the functionality at this position did not make contact with the enzyme surface but served to influence the overall physicochemical properties of the inhibitor.[15] These results were consolidated by the attainment of an enzyme-bound structure of **1** following soaking of the inhibitor into preformed crystals of the NS5B apoenzyme (Figure 1).[18] As anticipated, the inhibitor binds in the thumb domain, where it occupies a well-defined lipophilic site with the aromatic ring of the indole stacked against the side chain of P495. The cyclohexyl ring at the indole C3 position is buried deep in a lipophilic pocket where 84 Å^2 of the available 95 Å^2 of lipophilic contact surface area is engaged. The methine proton on the cyclohexyl ring is oriented toward the C2-phenyl ring of the inhibitor, which itself lies skewed to the plane of the indole (with a dihedral angle of −50.9°) and occupies a lipophilic channel. An electrostatic interaction between the carboxylic acid and arginine 503 is apparent, and in line with our expectation; the indole nitrogen atom is positioned such that the acetamide side chain is projected into a solvent-exposed region, little contact being made between this group and the enzyme. Interestingly, the three-dimensional structure of **1** that we observe is consistent with the preferred enzyme-bound conformation of a related benzimidazole inhibitor determined by NMR experiments,[10] adding weight to the expectation that these compounds bind at the same allosteric site on the NS5B enzyme.

On the basis of our initial SAR and the structure of **1** bound to the NS5B enzyme, we speculated that a strategy for improving the cell-based activity in this series would be the combinatorial optimization of the C2 position of the inhibitor together with the N1 acetamide moiety. As previously, improved intrinsic potency was targeted through enhanced contact of the ligand with the enzyme at C2, while structural changes at the acetamide group aimed to improve the physical

properties of the inhibitor (such as plasma protein binding) with a view to enhancing activity within the cell. To explore this strategy and to further extend our knowledge of the SAR around the indole core, a 10 × 50 compound array was designed. The building blocks for this work were indole-*N*-acetic acids **58** (Scheme 1) and were predominantly selected to incorporate small lipophilic substituents (e.g., **58b**) of the type found to be beneficial in our earlier studies. The inclusion of **58c** allowed evaluation of C5 carboxylic acid derivatives, and likewise, use of **58d** allowed the C3-cyclopentylindoles to be assessed. The 50 amines for the N1 dimension were chosen to broadly reflect three structural classes: (i) small alkylamines to provide inhibitors similar to the lead itself; (ii) diamines to provide inhibitors that are formally zwitterionic in nature, and (iii) electroneutral amines containing additional polar functionality (e.g., sulfone, sulfonamide, and amide) to favor inhibitors with reduced lipophilicity.

Compounds from this work were screened for cell-based activity at a fixed concentration of 5 μM, and IC_{50} and EC_{50} values were subsequently determined for compounds showing >50% inhibition in this primary screen. Subsets of the results, which broadly reflect the discoveries obtained from this array as a whole, are shown in Table 1. The data in columns 1 and 2 clearly highlight that changes to the indole-*N*-acetamide side chain did not significantly impact enzyme affinity, with flat SAR being observed for compounds **2**−**9** and **10**−**17**. However, the 4-chlorophenyl derivatives (column 2) consistently showed improved enzyme affinity over the corresponding phenyl analogues (column 1) and proved to be the most potent inhibitors found in this work. Submicromolar cell-based activity was rarely achieved when a simple dialkylacetamide or monoalkylacetamide was present at N1 (compounds **2**, **3**, **10**, and **11**). More surprisingly, the presence of polar functionality in the acetamide side chain (compounds **4**−**6** and **12**−**14**) also brought little benefit in terms of cell-based efficacy. Despite the use of amines containing structurally diverse polar functionality in this work, submicromolar cell-based activity was rarely observed and no significant improvement over the simple morpholine acetamide that is present in **1** itself was achieved. However, cell-based potency was consistently augmented when a basic amine was incorporated at N1, compounds **7**−**9** and **15**−**17** showing a 2- to 5-fold improvement over the corresponding dialkylacetamides **2** and **10** (which contain the same functionality at C2). The results in column 3 illustrate that indole-5-carboxylic acids lost around 10-fold potency with respect to the regioisomeric 6-carboxylic acids (column 1). A steric clash between the enzyme and the C5 carboxylic acid functionality (which apparently cannot be alleviated through a reorganized binding mode of the inhibitor driven by the electrostatic interaction with Arg503) is a likely explanation. The 3-cyclopentylindoles (column 4) showed only marginally weaker enzyme affinity than the corresponding cyclohexyl analogues and, at least in the presence of acetamides containing basic functionality, also showed comparable cell-based activity.

Since blockade of HCV replication after absorption of an NS5B inhibitor from the gastrointestinal tract will likely depend on the fraction of drug that is free to elicit

Table 1. IC$_{50}$ and EC$_{50}$ Values for Indole-*N*-acetamides Prepared as Part of a Two-Dimensional Array

		Column 1			Column 2			Column 3			Column 4	
X	No	[a,b]IC$_{50}$ (nM)	EC$_{50}$ (μM)	No	IC$_{50}$ (nM)	EC$_{50}$ (μM)	No	IC$_{50}$ (nM)	EC$_{50}$ (μM)	No	IC$_{50}$ (nM)	EC$_{50}$ (μM)
	2	62	1.6	**10**	11	0.9	**18**	[c]n.d.	>5	**26**	n.d.	>5
	3[d]	63	1.3	**11**	8	1.4	**19**	n.d.	>5	**27**	n.d.	>5
	4	98	1.9	**12**	17	1.1	**20**	n.d.	>5	**28**	n.d.	>5
	5	43	1.6	**13**	11	0.9	**21**	n.d.	>5	**29**	n.d.	>5
	6	19	0.9	**14**	7	0.5	**22**	n.d.	>5	**30**	n.d.	>5
	7	71	0.7	**15**	13	0.2	**23**	244	5.0	**31**	78	1.5
	8[d]	39	0.5	**16**	12	0.3	**24**	448	3.5	**32**	68	0.8
	9[d]	18	0.3	**17**[d]	12	0.3	**25**	n.d.	>5	**33**	47	0.4

[a] Compounds were initially tested in the replicon assay at a fixed concentration of 5 μM. IC$_{50}$ and EC$_{50}$ values were determined only for compounds showing >50% inhibition in this initial screen. [b] Unless otherwise stated, IC$_{50}$ and EC$_{50}$ values were determined in a single experiment. [c] n.d. = not determined. [d] IC$_{50}$ and EC$_{50}$ values are the arithmetic mean of multiple experiments. Standard errors or half-ranges are within 35% of the mean.

its pharmacological effect,[19] an attractive feature of indoles incorporating basic functionality in the acetamide side chain is their reduced binding to human serum proteins in the cell-based assay media. Thus, compound **9** retained low-micromolar activity (EC$_{50}$ = 1.5 ± 0.6 μM) when the cell-based assay was carried out in the presence of 50% normal human serum, while compound **14** (the best of the nonbasic acetamides discovered in the array) showed a 10-fold shift in potency (EC$_{50}$ = 5 μM). This trend held across a range of compounds from the above work, a low shift (<10-fold) from activity in our routine screen to high-serum conditions being seen only for compounds that incorporated basic functionality at N1. Formally zwitterionic inhibitors apparently offer an optimal compromise between human plasma protein binding (hPPB) and cell penetration. Thus, **9** (hPPB 96%) showed significantly lower human plasma protein binding than simple alkylacetamides such as **43** (Table 4, hPPB > 99%, EC$_{50}$ = 10 μM under high-serum conditions) and retains improved cell-based activity under high-serum conditions relative to acidic compounds such as **6** (EC$_{50}$ = 8 μM; hPPB = 97%) that have comparable intrinsic potency and plasma protein binding properties.

As a representative "zwitterionic" indole-*N*-acetamide, **9** was further characterized in in vivo and in vitro screens. The presence of basic functionality at N1 resulted in a substantially changed profile with respect to a previously reported indole-*N*-acetamide **43**.[15] In

Table 2. In Vivo Pharmacokinetic Properties for Indole-*N*-acetamide Inhibitors of the HCV NS5B Polymerase

[a]No.	Species	[b]Dose		[c]F (%)	[d]T$_{1/2}$ (h)	[e]Clp (mL/min/kg)
		p.o.	i.v.			
9	[f]Rat	3	3	1.9	1.5±0.2	51±9
	[g]Dog	2	[i]0.5	28±6	1.2	22
55	[h]Rat	3	3	10±3	3.1±1.0	44±11
	[g]Dog	2	1	51±19	5.0±0.8	9±2

[a] Compounds were dosed as trifluoroacetate salts. [b] mg/kg body weight; $n = 3$. [c] Oral bioavailability. [d] Terminal phase plasma half-life following iv administration. [e] Plasma clearance. [f] Vehicle iv 20% DMSO/80% PEG$_{400}$/20% H$_2$O, po PEG-400. [g] Male beagle, vehicle iv 20% DMSO/40% PEG-400/40% H$_2$O, po PEG-400. [h] Vehicle iv 20% DMSO/80% saline, po 50% PEG-400/50% H$_2$O. [i] $n = 2$

pharmacokinetic studies (Table 2), **9** showed low oral bioavailability in rat (F = 1.9%) and had both a rather short plasma half-life (1.5 h) and a high plasma clearance (51 mL min^{-1} kg^{-1}). The oral bioavailability was somewhat improved in dog (F = 28%), but again, the half-life was short (1.2 h). Counterscreening studies showed that **9** did not inhibit human DNA polymerases[11] α, β, and γ, but potent activation of the nuclear pregnane X receptor[20] (PXR) was identified as

Chart 1. PXR Activation[a]

9
82% @ 10 μM

35
14% @ 10 μM

34
72% @ 10 μM

36
30% @ 10 μM

17
92% @ 10 μM

37
15% @ 10 μM
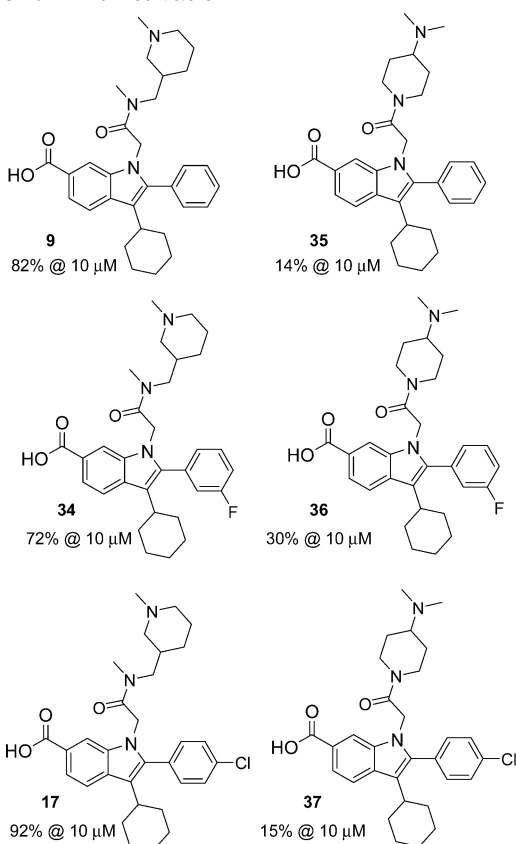
[a] Results are expressed as % PXR mediated induction of the SEAP reporter gene with respect to positive control (10 μM rifampicin).

Table 3. IC_{50} and EC_{50} Values for Inhibitors with Nonaromatic Functionality at the C2 Position of the Indole

No.	X	[a]IC_{50} (nM)	[b]EC_{50} (μM)
35	Ph	41±17	0.3±0.01
38	$-CH_2CH_3$	[d]283	[c]n.d.
39	cyclohexyl	72±6	4.0±0.9
40	$-CHCH_2$	49±15	2.8±1.3
41	1-cyclohexenyl	18±3	[d]0.4
42	$-CCH$	[d]228	n.d.

[a] IC_{50} and EC_{50} values are the arithmetic mean ± half-range (or standard error) for a minimum of two independent determinations. [b] Assay run in the presence of 10% fetal calf serum. [c] n.d. = not determined. [d] $n = 1$.

an off-target activity. PXR activation is associated with induction of cytochrome P450 (CYP) 3A4 and was a particular liability for **9** because CYP3A4 was also found to mediate its oxidative metabolism (in human liver microsomes). The potential of the compound to induce the CYP3A4 gene was of concern because of the potential for drug−drug interactions and nonlinear pharmacokinetics for inhibitors with this profile. To assess whether PXR activation was compound-specific or was a feature of "zwitterionic" indoles in general, a range of compounds were assayed. The availability of compounds prepared as part of a two-dimensional array proved to be invaluable in facilitating our understanding of this issue; PXR activation was closely correlated to the structure of the acetamide side chain attached at N1. Thus, the presence of the acetamide found in **9** also led to a high level of PXR activation in compounds **17** and **34** (Chart 1). In contrast, compounds **35−37** showed low PXR activation with respect to the positive control, demonstrating that this off-target activity is not an inherent liability for this structural class.

With a view to further enhancing the potency of **9**, extensive explorations at the C2 region of the indole (which had been the less explored dimension in our initial array) were performed. Alternatives to aromatic functionality at C2 were evaluated in the presence of an *N*-acetamide that contained a basic amine (Table 3). The hybridization at the carbon atom directly attached to the indole ring proved to be important with regard to enzyme affinity. Simple sp- or sp³-hybridized groups, the ethynyl derivative **42** and the ethyl compound **38**, respectively, showed poor affinity for NS5B. The cy-
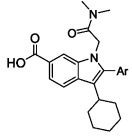
cloalkyl functionality (**39**) resulted in enzyme inhibition comparable to that of the corresponding phenyl compound **35** but gave much poorer cell-based activity. The presence of sp²-hybridized functionality directly attached to the indole provided the best alternative to aromatic groups, the vinyl compound **40** being 7-fold more active than either the corresponding ethyl or ethynyl derivative and showing enzyme affinity similar to that of the C2-phenylindole **35**. A further gain was achieved with the 1-cyclohexenyl compound **41** that was comparable to **35** in both the enzyme and replicon assays.

In view of the attractive characteristics of formally zwitterionic compounds, the attachment of basic functionality at alternative positions around the inhibitor was explored. Our evaluation of compounds incorporating basic amines pendant to the C2 phenyl ring along with a simple dimethylacetamide at N1 is shown in Table 4. The presence of the *N,N*-dimethylaminomethyl functionality at the 4-position of the phenyl ring resulted in weak enzyme inhibition (compound **44**). More potent activity was possible through positioning of the basic functionality at the 3-position of the aromatic ring, though **45** remained 2- to 3-fold weaker in both the enzyme and cell-based assays than the simple phenyl compound **43**. The combination of basic functionality in the meta position and the potency-enhancing para-Cl substituent that had emerged from our previous work led to a rather modest gain in this setting, with compound **46** showing no real advantage over **45**. Somewhat improved affinity was also achieved with more lipophilic amines such as **47**, and a feature of these compounds was the very low shift between standard and high-serum conditions in the cell-based assay. Thus, **47** was essentially equipotent in the presence of NHS (EC_{50} = 1.8 μM) as in our routine screen (EC_{50} = 1.1 μM), an observation in line with the lower binding to human plasma proteins shown by inhibitors of this type (**47**

Table 4. IC$_{50}$ and EC$_{50}$ Values for Inhibitors with Basic Amine Functionality Attached to the C2-Phenyl Substituent of the Indole
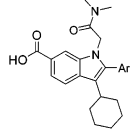

No.	Ar	[a]IC$_{50}$ (nM)	[b]EC$_{50}$ (μM)
43		59±6	1.5±0.6
44		[c]920	[c]17.6
45		147±5	3.3±0.5
46		78±1	2.7±0.2
47		78±2	1.1±0.2
48		18±1	0.6±0.1

[a] IC$_{50}$ and EC$_{50}$ values are the arithmetic mean ± half range (or standard error) for a minimum of two independent determinations. [b] Assay run in the presence of 10% fetal calf serum. [c] $n = 1$.

hPPB = 84%). Ultimately, however, while the activity of **47** in high-serum conditions compared favorably with compounds such as **9**, we were unable to further improve potency in this area without recourse to highly lipophilic functionality. Compound **48** provided the most active inhibitor of this type in our routine assays, but high plasma protein binding (hPPB = 99%) and serum shift (8-fold) were unattractive with a view to further optimization.
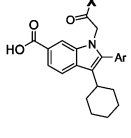
Polar heterocycles such as pyridine were attractive alternatives to the C2 phenyl ring of **1** with a view to reduced overall lipophilicity, but both the 3- and 4-pyridines (**49** and **50**, respectively, Table 5) showed reduced enzyme affinity over **43**. Gains were again achieved through introduction of functionality that had previously brought improved potency in the phenyl series (e.g., 4-OMe, **51**), though such compounds offered no advantage over **43** in terms of cell-based potency. These results, together with work performed in a related series (data not shown), established that basic and nonbasic electron-deficient heterocycles are suboptimal at C2. In contrast, electron-rich heteroaromatics such as 3-furan **52** provided a modest gain in enzyme affinity and cell-based efficacy with respect to the corresponding phenyl analogue.

Inhibitors with increased cell-based activity over **9** and with an improved overall profile ultimately arose from extensive efforts combining the optimal substituents that we had found at C2 with structurally diverse acetamides containing a basic amine (Table 6). This work was largely empirical in nature with few trends

Table 5. IC$_{50}$ and EC$_{50}$ Values for Inhibitors with Heterocyclic Functionality at the C2 Position of the Indole

No.	Ar	[a]IC$_{50}$ (nM)	[b]EC$_{50}$ (μM)
43		59±6	1.5±0.6
49		[c]332	[c]13.0
50		134±44	[c]6.7
51		69±12	1.8±0.1
52		31±1	0.8±0.1

[a] IC$_{50}$ and EC$_{50}$ values are the arithmetic mean ± half-range (or standard error) for a minimum of two independent determinations. [b] Assay run in the presence of 10% fetal calf serum. [c] $n = 1$.

Table 6. Cell-Based Activities under Standard and High-Serum Conditions for Optimized Indole-*N*-acetamide Inhibitors of the HCV NS5B Polymerase

[a]No.	X	Ar	[b]EC$_{50}$ (nM) [c]Standard Conditions	[b]EC$_{50}$ (nM) [d]High Serum
53			158±19	677±52
54			[f]144±14	[f]422±98
55			[f]127±23	[f]454±112
56			199±2	633±6
[e]57			152±8	376±40

[a] Compounds **53**−**57** had IC$_{50}$ values between 6 and 9 nM after measurement in duplicate. Half-ranges were within 20% of the arithmetic mean. [b] EC$_{50}$ values are the arithmetic mean ± half-range (or standard error) for a minimum of two independent determinations. [c] Assay run in the presence of 10% fetal calf serum. [d] Assay run in the presence of 50% normal human serum. [e] Racemic. [f] $n = 5$

in the SAR appearing, and it may be considered an optimization of plasma protein binding in tandem with intrinsic potency. Lipophilic tertiary basic amines were generally preferred (compound **54** vs **53**; compound **55**

was also 2-fold more potent than **37**), and though the results in Table 6 reflect our preference for achiral inhibitors, potent cell-based activity was achievable with structurally diverse acetamides (**53** vs **57**). All compounds in Table 6 showed sub-10 nM potency against the ΔC_{55} NS5B polymerase and retained strong affinity for the ΔC_{21} enzyme (e.g. **57** IC_{50} = 21 nM). Under our routine screening conditions, compounds **53**−**57** had activities in the 100−200 nM range in the cell-based assay and showed low cytotoxicity[11] toward the HUH-7 cells (e.g., compound **57** showed 5% toxicity at 15 μM; CC_{50} not determined). A modest drop in potency (2- to 3-fold) was observed in the presence of human serum, with compounds **54**, **55**, and **57** retaining potency in the sub-500 nM range. Compound **55** was further profiled and showed no activity (at 10 μM) in human PXR-dependent reporter gene assays, suggesting that it has little potential to cause drug−drug interactions or autoinduction of metabolism in humans. The compound also showed no inhibition of human DNA polymerases[11] and no off-target activities in extensive counterscreening efforts.[21] The rat pharmacokinetic (PK) profile (Table 2) of **55** was somewhat improved with respect to **9**, though oral bioavailability remained rather low (F = 10%). Interestingly, despite its modest systemic exposure, a high concentration of **55** (0.5 μM) was found in homogenates of rat liver (the main target organ for an anti-HCV agent) 6 h after oral administration (3 mpk). In dog, **55** had both good oral bioavailability (F = 51%) and a plasma half-life ($T_{1/2}$ = 5 h) that was much improved over that of **9** ($T_{1/2}$ = 1.2 h).

In our early studies toward optimizing **43** (our original lead in the indole-*N*-acetamide area), we found that introduction of a 4-benzyloxy substituent on the C2-phenyl ring of the inhibitor gave a 10-fold improvement in enzyme affinity.[15] However, the cell-based activity for this compound was *diminished* compared to **43**. In the present report we have described efforts that aimed to align improved enzyme affinity with physicochemical properties that favor cell-based potency. The most active molecule here described (**57**, EC_{50} = 0.15 μM) is again a 10-fold more potent enzyme inhibitor than **43** and additionally shows a parallel improvement in cell-based activity in our routine screen (**43**, EC_{50} = 1.5 μM). Furthermore, a 20- to 30-fold improvement in cell-based activity in the presence of human serum has been achieved. Under these conditions, which may be considered a more physiologically relevant assay system,[19] **43** is a weak inhibitor (EC_{50} = 10 μM) while **57** (EC_{50} = 376 nM) retains strong submicromolar potency. A comparison of **57** with the HCV NS3 protease inhibitor BILN2061[22] provides insight to the potential of this series of compounds as antiviral agents. Phase I clinical data for BILN2061 has demonstrated that a strong (2 log) reduction in viral load can be achieved after its administration to patients infected with genotype 1 virus.[7] In our hands, BILN2061 showed an EC_{50} of 131 nM when the replicon assay was run under high-serum conditions. Compound **57** shows a similar (within 2- to 3-fold) blockade of subgenomic HCV RNA replication under these conditions, and although the biochemical targets for **57** and BILN2061 are different, these data suggest that their overall physiological effect may well prove to be similar.

Conclusions

In this report we have summarized our efforts toward the optimization of indole-*N*-acetamide inhibitors of the NS5B polymerase. A library-based approach toward exploration of SAR initially brought a 5-fold improvement in intracellular activity and firmly established that formally zwitterionic inhibitors such as **9** were necessary for potent blockade of HCV subgenomic RNA replication in the replicon assay. The only significant off-target activity for this type of compound (PXR activation) can be avoided through appropriate selection of the acetamide group attached to the indole N1 atom. Optimization of **9** provided compounds such as **54**, **55**, and **57** that show strong potency in the cell-based assay under routine conditions and in the presence of a high concentration of human serum. Compound **55** shows encouraging PK properties in both rat and dog and is clean in an extensive panel of counterscreening assays. This profile, together with the comparable efficacy shown by **55** and BILN2061 when the replicon assay is performed in the presence of human serum, highlights the potential of this structural series for the development of novel anti-HCV agents.

Experimental Section

Solvents (Fluka, puriss. grade) were obtained from commercial suppliers and were used without further purification. Solid-phase reagents and scavenger resins were purchased from Argonaut and were used without confirmation of loadings. Organic extracts were dried over anhydrous sodium sulfate (Merck). Flash chromatography purifications were performed using 230−400 mesh silica gel 60 (Merck) as the stationary phase or were conducted using prepacked Isolute Si cartridges on a Flashmaster Personal system. NMR spectra were recorded on Bruker AM series spectrometers and unless otherwise stated were recorded at 300 K and 300 MHz. Chemical shifts for observed signals are reported in parts per million downfield from tetramethylsilane and are measured using the residual resonance from the deuterated solvent as reference. Preparative scale reversed-phase high-performance liquid chromatography (RP-HPLC) was performed on a Thermoquest AP2000 system operating with a flow rate of 20 mL/min and incorporating a UV1000 absorption module operating at 254 nm. The stationary phases used were Waters Symmetry C_{18} 5 μm, 19 mm × 100 mm (column A); Waters Symmetry C_{18} 5 μm, 19 mm × 50 mm (column B); Waters Xterra 5 μm, 19 mm × 100 mm (column C); Waters Symmetry C_{18} 7 μm, 19 mm × 300 mm (column D). The mobile phase comprised a linear gradient of binary mixtures of MeCN (containing 0.1% TFA) (solvent A) and H_2O (containing 0.1% TFA) (solvent B). The conditions used were as follows: 10% solvent A (2 min) to 90% solvent A over 10 min, column A (method 1); 10% solvent A (1 min) to 100% solvent A over 5 min, column 2 (method 2); 25% solvent A (1 min) to 50% solvent A over 11 min, column A (method 3); 10% solvent A (2 min) to 90% solvent A over 20 min and then isocratic, column C (method 4); 10% solvent A (2 min) to 90% solvent A over 20 min and then isocratic, column D (method 5). Automated (mass-triggered) RP-HPLC purifications were performed using a Waters Micromass system incorporating a 2525 pump module, a Micromass ZMD detector, and a 2767 collection module, operating under Fraction Lynx software. The stationary phase used was column C, and the flow rate was 20 mL/min. Analytical scale RP-HPLC was performed using the mobile phases described above and the following conditions: 10% solvent A (1 min) to 100% solvent A over 8 min and then isocratic; stationary phase, Waters Symmetry C_{18} (150 mm × 4.6 mm, 5 μm); flow rate, 1 mL/min (method 1); 30% solvent A (1 min) to 90% solvent A over 8 min and then isocratic; stationary phase, Waters Xterra C_{18} (150 mm × 3.0 mm, 5 μm); flow rate, 1 mL/min (method 2). Accurate mass determi-

nations were performed on a Finnegans TSQ-AM triple quadropole system operating with a Surveyor pump and a CTC-PAL autosampler.

Parallel Synthesis of Compounds 2−37. General Procedure. Chromacol tubes were charged with PS-carbodiimide resin (127 mg, loading 0.9 mmol/g) and then treated with a 0.038 M solution of the indole-*N*-acetic acids **58** (1 mL, 0.038 mmol). The tubes were capped, then agitated on a vortex mixer for 0.5 min. The appropriate amine added as a 0.09 M solution (1 mL, 0.09 mmol) in CH$_2$Cl$_2$. The tubes were again agitated as previously, then were tightly sealed with a screw cap and attached to a rotor for 24 h. PS-NCO resin (143 mg, loading 1.6 mmol/g, 0.22 mmol) was added, and after agitation on a vortex mixer, the tubes were attached for a further 24 h to a rotor. The reaction mixtures were then filtered through a fritted syringe, the resins were washed with CH$_2$Cl$_2$ (2 × 1 mL), and the combined filtrates were collected in a second series of chromacol tubes. These were treated with a freshly prepared solution of BBr$_3$ (1.5 M in CH$_2$Cl$_2$, 0.1 mL, 0.15 mmol) and then shaken for 20 min. H$_2$O (0.1 mL) was added, and the volatiles were removed under reduced pressure (Savant speed vacuum). The residues were dissolved by addition of MeCN (and DMSO where necessary). Purification by RP-HPLC (method 2) or by Fraction-Lynx automated RP-HPLC or by filtration through a preconditioned Isolute C$_{18}$ SPE cartridge (2 g) using 2:8 MeCN (containing 0.1% TFA)/H$_2$O (containing 0.1% TFA) as eluent afforded the desired inhibitors **2−37**.

3-Cyclohexyl-1-(2-{methyl[(1-methylpiperidin-3-yl)methyl]amino}-2-oxoethyl)-2-phenyl-1*H*-indole-6-carboxylic Acid Trifluoroacetate (9). Following the general procedure described above, treatment of **58a** with [(1-methylpiperidin-3-yl)methyl]amine followed by purification by RP-HPLC (method 2) afforded the title compound (8.6 mg, 36%). ^{1}H NMR (DMSO-d_6, 340 K) δ 1.13−1.41 (m, 3H), 1.47−1.97 (m, 11H), 1.97−2.19 (m, 1H), 2.57−2.71 (m, 1H), 2.78 (s, 3H), 2.94 (s, 3H), 3.04−3.36 (m, 6H), 4.92 (s, 2H), 7.33−7.50 (m, 2H), 7.53−7.65 (m, 3H), 7.73 (d, *J* = 8.2 Hz, 1H), 7.86 (d, *J* = 8.2 Hz, 1H), 8.00 (br s, 1H); MS (ES$^+$) *m/z* 502 (M + H)$^+$; RP-HPLC method 1, t_R = 7.1 min (>99%); method 2, t_R = 7.31 (96%).

1-[(6-Carboxy-3-cyclohexyl-2-ethyl-1*H*-indol-1-yl)acetyl]-*N,N*-dimethylpiperidin-4-aminium Trifluoroacetate (38). A solution of **40** (8 mg, 0.015 mmol) in MeOH (3 mL) was treated with 10% Pd/C (1 mg) and the mixture was stirred under an atmosphere of hydrogen for 12 h. The mixture was filetered and concentrated in vacuo. The residue was purified by RP-HPLC (Fraction-Lynx) to afford the title compound (4 mg, 48%) as a solid. ^{1}H NMR (400 MHz, DMSO-d_6) δ 1.08 (t, *J* = 7.7 Hz, 3H), 1.32−1.52 (m, 4H), 1.63−1.78 (m, 4H), 1.80−1.98 (m, 4H), 1.99−2.09 (m, 1H), 2.09−2.20 (m, 2H), 2.59−2.67 (m, 1H), 2.69 (q, *J* = 7.7 Hz, 2H), 2.80 (d, *J* = 4.6 Hz, 6H), 3.13−3.25 (m, 1H), 3.45−3.60 (m, 1H), 4.24−4.35 (m, 1H), 4.40−4.50 (m, 1H), 5.10−5.31 (m, 2H), 7.57 (d, *J* = 8.3 Hz, 1H), 7.69 (d, *J* = 8.3 Hz, 1H), 7.85 (s, 1H), 9.71 (br s, 1H), 12.39 (br s, 1H); MS (ES$^+$) *m/z* 440 (M + H)$^+$; RP-HPLC method 1, t_R = 6.6 min (>99%); method 2, t_R = 5.4 (>98%).

1-[(6-Carboxy-2,3-dicyclohexyl-1*H*-indol-1-yl)acetyl]-*N,N*-dimethylpiperidin-4-aminium Trifluoroacetate (39). A solution of methyl 2-cyclohex-1-en-1-yl-3-cyclohexyl-1-{2-[4-(dimethylamino)piperidin-1-yl]-2-oxoethyl}-1*H*-indole-6-carboxylate (33 mg, 0.065 mmol) in MeOH was treated with 10% Pd/C (20 mg), and the reaction mixture was stirred under hydrogen for 12 h. The catalyst was filtered off, and the solvent was removed to afford methyl 2,3-dicyclohexyl-1-{2-[4-(dimethylamino)piperidin-1-yl]-2-oxoethyl}-1*H*-indole-6-carboxylate (30 mg, 91%) as a solid. This material was hydrolyzed as described for **41**, then purified by RP-HPLC (method 1) to give the title compound (20 mg, 58%) as a white solid. ^{1}H NMR (400 MHz, DMSO-d_6) δ 1.24−1.35 (m, 3H), 1.35−1.49 (m, 4H), 1.58−1.89 (m, 13H), 1.89−2.22 (m, 4H), 2.57−2.71 (m, 2H), 2.80 (d, *J* = 4.2 Hz, 6H), 2.94−3.06 (m, 1H), 3.12−3.25 (m, 1H), 3.44−3.46 (m, 1H), 4.28−4.42 (m, 2H), 5.15−5.40 (m, 2H), 7.55 (d, *J* = 8.3 Hz, 1H), 7.71 (d, *J* = 8.3 Hz, 1H), 7.89 (s, 1H), 8.90 (br s, 1H), 12.41 (br s, 1H); MS (ES$^+$) *m/z* 494 (M + H)$^+$;

RP-HPLC method 1, t_R = 7.4 min (>99%); method 2, t_R = 6.4 (>99%).

1-[(6-Carboxy-3-cyclohexyl-2-vinyl-1*H*-indol-1-yl)acetyl]-*N,N*-dimethylpiperidin-4-aminium Trifluoroacetate (40). A solution of methyl 2-bromo-3-cyclohexyl-1-{2-[4-(dimethylamino)piperidin-1-yl]-2-oxoethyl}-1*H*-indole-6-carboxylate (1.4 g, 4.16 mmol) in dioxane (25 mL) was treated with tributyl(vinyl)stannane (1.4 g, 4.45 mmol). PdCl$_2$(PPh$_3$)$_2$ (292 mg, 0.42 mmol) was added, and the reaction mixture was degassed and then stirred at 100 °C for 1 h. The mixture was diluted with EtOAc and then washed with H$_2$O and brine. The dried organic layer was concentrated and the residue was purified by flash chromatography (1:9 EtOAc/petroleum ether) to afford methyl 3-cyclohexyl-2-vinyl-1*H*-indole-6-carboxylate (0.88 g, 75%). A portion of this material (116 mg, 0.26 mmol) was hydrolyzed as described for **41**. Purification of the resulting residue by RP-HPLC (method 1) afforded the title compound (54 mg, 38%) as a solid. ^{1}H NMR (400 MHz, DMSO-d_6) δ 1.28−1.53 (m, 4H), 1.58−1.79 (m, 4H), 1.79−1.89 (m, 2H), 1.89−2.18 (m, 4H), 2.59−2.72 (m, 1H), 2.79 (d, *J* = 4.2 Hz, 6H), 2.87−3.00 (m, 1H), 3.09−3.22 (m, 1H), 3.42−3.56 (m, 1H), 4.16−4.29 (m, 1H), 4.39−4.51 (m, 1H), 5.11−5.32 (m, 2H), 5.42 (dd, *J* = 17.9, *J* = 1.1 Hz, 1H), 5.62 (dd, *J* = 11.4, 1.1 Hz, 1H), 6.77 (dd, *J* = 17.9, 11.4 Hz, 1H), 7.60 (d, *J* = 8.3 Hz, 1H), 7.81 (d, *J* = 8.3 Hz, 1H), 7.93 (s, 1H), 9.62 (br s, 1H), 12.53 (br s, 1H); MS (ES$^+$) *m/z* 438 (M + H)$^+$; RP-HPLC method 1, t_R = 6.6 min (95%); method 2, t_R = 5.4 (96%).

1-[(6-Carboxy-2-cyclohex-1-en-1-yl-3-cyclohexyl-1*H*-indol-1-yl)acetyl]-*N,N*-dimethylpiperidin-4-aminium Trifluoroacetate (41). Step 1. A solution of methyl 2-bromo-3-cyclohexyl-1-{2-[4-(dimethylamino)piperidin-1-yl]-2-oxoethyl}-1*H*-indole-6-carboxylate (100 mg, 0.20 mmol) in 1,4-dioxane (4 mL) was treated with 2-cyclohex-1-en-1-yl-4,4,5,5-tetramethyl-1,3,2-dioxaborolane (124 mg, 0.6 mmol) and Na$_2$CO$_3$ (105 mg, 0.99 mmol). Pd(PPh$_3$)$_2$Cl$_2$ (28 mg, 0.04 mmol) was added, and the reaction mixture was stirred at 80 °C for 20 min. The mixture was cooled and then diluted with EtOAc and washed with brine. The dried organic layer was concentrated and the residue was purified by flash chromatography (3:97 MeOH/CH$_2$Cl$_2$) to afford methyl 2-cyclohex-1-en-1-yl-3-cyclohexyl-1-{2-[4-(dimethylamino)piperidin-1-yl]-2-oxoethyl}-1*H*-indole-6-carboxylate (68 mg, 68%).

Step 2: General Procedure for Ester Hydrolysis. A portion of the material from above (59 mg, 0.12 mmol) in a 1:1 mixture of dioxane and H$_2$O was treated with aqueous KOH (1 N, 0.35 mL, 0.35 mmol) and stirred at 70 °C for 24 h. The mixture was cooled, the volatiles were removed in vacuo, and the residue was treated with aqueous HCl (1 N). The solid obtained was dissolved by addition of MeCN, H$_2$O, and a minimal amount of DMSO. Purification by RP-HPLC gave the title compound (30 mg, 42%) as a white solid. ^{1}H NMR (400 MHz, DMSO-d_6) δ 1.23−1.46 (m, 5H), 1.48−1.62 (m, 1H), 1.62−1.77 (m, 7H), 1.77−1.94 (m, 4H), 2.00−2.24 (m, 6H), 2.56−2.72 (m, 2H), 2.79 (d, *J* = 4.3 Hz, 6H), 3.08−3.20 (m, 1H), 4.18−4.29 (m, 1H), 4.40−4.51 (m, 1H), 5.03 (s, 2H), 5.72−5.78 (m, 1H), 7.59 (d, *J* = 8.3 Hz, 1H), 7.71 (d, *J* = 8.3 Hz, 1H), 7.87 (s, 1H), 9.83 (br s, 1H), 12.47 (br s, 1H); MS (ES$^+$) *m/z* 492 (M + H)$^+$; RP-HPLC method 1, t_R = 7.3 min (>98%); method 2, t_R = 6.3 (>99%).

1-[(6-Carboxy-3-cyclohexyl-2-ethynyl-1*H*-indol-1-yl)acetyl]-*N,N*-dimethylpiperidin-4-aminium Trifluoroacetate (42). A solution of methyl 2-bromo-3-cyclohexyl-1-{2-[4-(dimethylamino)piperidin-1-yl]-2-oxoethyl}-1*H*-indole-6-carboxylate (150 mg, 0.30 mmol) in Et$_3$N (3 mL) was treated with ethynyl(trimethyl)silane (44 mg, 0.45 mmol) and Pd(PPh$_3$)$_4$ (35 mg, 0.030 mmol). CuI (11 mg, 0.06 mmol) was added, and the reaction mixture was stirred in a sealed tube at 90 °C for 6 h. The mixture was diluted with EtOAc and then washed with H$_2$O and brine. The dried organic layer was concentrated, and the residue was purified by flash chromatography (3:97 MeOH/CH$_2$Cl$_2$) to afford methyl 3-cyclohexyl-1-{2-[4-(dimethylamino)piperidin-1-yl]-2-oxoethyl}-2-[(trimethylsilyl)ethynyl]-1*H*-indole-6-carboxylate (51 mg, 33%). Hydrolysis of this material as described for **41** followed by RP-HPLC (method 1) afforded the

title compound (7 mg, 13%) as a white solid. ^{1}H NMR (400 MHz, DMSO-d_6) δ 1.26−1.52 (m, 4H), 1.56−1.71 (m, 1H), 1.71−1.81 (m, 3H), 1.81−1.98 (m, 4H), 1.99−2.09 (m, 1H), 2.09−2.18 (m, 1H), 2.59−2.71 (m, 1H), 2.79 (d, J = 4.6 Hz, 6H), 2.90−3.02 (m, 1H), 3.09−3.25 (m, 1H), 3.40−3.52 (m, 1H), 4.19−4.31 (m, 1H), 4.38−4.50 (m, 1H), 4.88 (s, 1H), 5.18−5.38 (m, 2H), 7.63 (d, J = 8.5 Hz, 1H), 7.78 (d, J = 8.5 Hz, 1H), 7.97 (s, 1H), 9.72 (br s, 1H), 12.65 (br s, 1H); MS (ES$^+$) m/z 436 (M + H)$^+$; RP-HPLC method 1, t_R = 6.5 min (>98%); method 2, t_R = 5.27 (>99%).

3-Cyclohexyl-2-{3-[(dimethylamino)methyl]phenyl}-1-[2-(dimethylamino)-2-oxoethyl]-1H-indole-6-carboxylic Acid Trifluoroacetate (45). Step 1. Following the general procedure described for **55**, treatment of methyl 2-bromo-3-cyclohexyl-1-[2-(dimethylamino)-2-oxoethyl]-1H-indole-6-carboxylate[15] (1.00 g, 2.37 mmol) with (3-formylphenyl)boronic acid (0.43 g, 2.85 mmol) afforded a residue that was purified by flash chromatography (5:5 to 7:5 EtOAc/petroleum ether) to give methyl 3-cyclohexyl-1-[2-(dimethylamino)-2-oxoethyl]-2-(3-formylphenyl)-1H-indole-6-carboxylate (0.73 g, 75%) as a solid. ^{1}H NMR (DMSO-d_6) δ 1.10−1.40 (m, 3H), 1.60−1.92 (m, 7H), 2.45−2.61 (m, 1H), 2.80 (s, 3H), 2.89 (s, 3H), 3.89 (s, 3H), 4.94 (s, 2H), 7.63−7.72 (m, 2H), 7.79 (t, J = 7.8 Hz, 1H), 7.84 (s, 1H), 7.90 (d, J = 8.4 Hz, 1H), 8.02−8.10 (m, 2H), 10.10 (s, 1H).

Step 2. A solution of the material from above (33 mg, 0.074 mmol) in 1,2-dichloroethane (3 mL) was treated with Et$_3$N (12 μL, 0.09 mmol), Na(OAc)$_3$BH (20 mg, 0.10 mmol), and Me$_2$-NH·HCl (6 mg, 0.08 mmol). The mixture was stirred for 5 h and then diluted with EtOAc and washed with saturated aqueous NaHCO$_3$ and brine. The dried organic phase was concentrated, then the residue was taken up in CH$_2$Cl$_2$ (3 mL) and treated with BBr$_3$ (0.021 mL, 0.22 mmol). The mixture was stirred for 3 h, and then the reaction was quenched with H$_2$O. The volatiles were removed under reduced pressure and the residue was purified by RP-HPLC (method 1) to give the title compound (22 mg, 64%) as a solid. ^{1}H NMR (DMSO-d_6) δ 1.11−1.42 (m, 3H), 1.61−2.01 (m, 7H), 2.52 (under DMSO, 1H), 2.78 (s, 3H), 2.78 (s, 6H), 2.91 (s, 3H), 4.38 (s, 2H), 4.93 (s, 2H), 7.42−7.49 (m, 2H), 7.61−7.67 (m, 2H), 7.68 (d, J = 8.4 Hz, 1H), 7.85 (d, J = 8.4 Hz, 1H), 8.00 (s, 1H), 9.85 (br s, 1H); MS (ES$^+$) m/z 462 (M + H)$^+$; RP-HPLC method 1, t_R = 6.2 min (>97%); method 2, t_R = 4.8 (>97%).

2-{4-Chloro-3-[(dimethylamino)methyl]phenyl}-3-cyclohexyl-1-[2-(dimethylamino)-2-oxoethyl]-1H-indole-6-carboxylic Acid Trifluoroacetate (46). Step 1. A solution of **61** (0.39 g, 0.60 mmol) in dioxane (12 mL) was treated with (5-bromo-2-chlorobenzyl)dimethylamine (0.30 g, 1.21 mmol), and CsF (0.81 g, 5.31 mmol) was added. The mixture was degassed and then treated with Pd$_2$(dba)$_3$ (54 mg, 0.06 mmol) and a solution of P^{t}Bu$_3$ (0.8 M) in dioxane (0.30 mL, 0.24 mmol). The mixture was degassed again and then heated under reflux for 12 h. The mixture was cooled, diluted with EtOAc, and washed with H$_2$O. The organic phase was separated, dried, and concentrated to give a residue that was purified by flash chromatography (5:95:0.1 EtOAc/petroleum ether/Et$_3$N) to afford a solid. This material was dissolved in CH$_2$Cl$_2$ (1.5 mL) and then treated with TFA (1.5 mL). The mixture was stirred for 1 h and then concentrated under reduced pressure. The residue was triturated with Et$_2$O to afford methyl 2-{4-chloro-3-[(dimethylamino)methyl]phenyl}-3-cyclohexyl-1H-indole-6-carboxylate (0.12 g, 35% yield). ^{1}H NMR (DMSO-d_6) δ 1.20−1.51 (m, 3H), 1.65−1.91 (m, 5H), 1.95−2.15 (m, 2H), 2.71−2.90 (m, 1H), 2.90 (s, 6H), 3.87 (s, 3H), 4.53 (s, 2H), 7.60−7.70 (m, 2H), 7.77−7.84 (m, 2H), 7.90 (d, J = 8.6 Hz, 1H), 8.03 (s, 1H); MS (ES$^+$) m/z 425 (M + H)$^+$.

Step 2. The material from above (60 mg, 0.11 mmol) in DMF (2 mL) was treated with Et$_3$N (0.032 mL, 0.23 mmol) and NaH as a mineral oil dispersion (60 wt %, 11 mg, 0.286 mmol). After 40 min, 2-chloro-N,N-dimethylacetamide (0.016 mL, 0.159 mmol) was added and the mixture was stirred for 12 h. Then the reaction was quenched with H$_2$O. The mixture was diluted with EtOAc, the layers were separated, and the organic phase was washed with H$_2$O and brine. The dried organic phase was

concentrated, and the residue was taken up in CH$_2$Cl$_2$ (2 mL) and treated with BBr$_3$ (0.032 mL, 0.34 mmol). After 20 min the reaction was quenched with H$_2$O. The mixture was dissolved in MeCN/DMSO and purified by RP-HPLC (method 3) to give the title compound (8 mg, 15%) as a white solid. ^{1}H NMR (DMSO-d_6) δ 1.10−1.41 (m, 3H), 1.59−1.95 (m, 7H), 2.52 (under DMSO, 1H), 2.78 (s, 3H), 2.78 (s, 6H), 2.94 (s, 3H) 4.35−4.50 (m, 2H), 4.90−4.99 (m, 2H), 7.43 (d, J = 7.9 Hz, 1H), 7.58 (s, 1H), 7.67 (d, J = 8.2 Hz, 1H), 7.75 (d, J = 7.9 Hz, 1H), 7.85 (d, J = 8.2 Hz, 1H), 7.99 (s, 1H); MS (ES$^+$) m/z 496 (M + H)$^+$; RP-HPLC method 1, t_R = 6.4 min (>99%); method 2, t_R = 5.1 (>99%).

1-{6-Carboxy-3-cyclohexyl-2-(4-methoxyphenyl)-1H-indol-1-yl]acetyl}-N,N-dimethylpiperidin-4-aminium Trifluoroacetate (53). Step 1: General Procedure for Solution-Phase Amide Couplings. A solution of [2-bromo-3-cyclohexyl-6-(methoxycarbonyl)-1H-indol-1-yl]acetic acid (2.0 g, 5.1 mmol) in CH$_2$Cl$_2$ (20 mL) was treated with N,N-dimethylpiperidin-4-amine bis(trifluoroacetate) (2.71 g, 7.6 mmol), DIEA (2.62 g, 20.3 mmol), and HATU (2.89 g, 7.6 mmol). The mixture was stirred for 12 h and then diluted with CH$_2$Cl$_2$ and washed sequentially with aqueous NaOH (1 N) and brine. The dried organic layer was concentrated in vacuo to afford a residue that was purified by flash chromatography (95:5 CH$_2$Cl$_2$/MeOH) to give methyl 2-bromo-3-cyclohexyl-1-{2-[4-(dimethylamino)piperidin-1-yl]-2-oxoethyl}-1H-indole-6-carboxylate (1.8 g, 70%) as a solid. ^{1}H NMR (DMSO-d_6) δ 1.15−1.25 (m, 8H), 1.70−2.10 (m, 7H), 2.41 (s, 6H), 2.60−2.78 (m, 1H), 2.80−2.93 (m, 1H), 3.10−3.23 (m, 1H), 3.89 (s, 3H), 4.07−4.20 (m, 1H), 4.22−4.38 (m, 1H), 5.20−5.42 (m, 2H), 7.67 (d, J = 8.3 Hz, 1H), 7.80 (d, J = 8.3 Hz, 1H), 8.02 (s, 1H).

Step 2. Following the general procedure described for **55**, treatment of a portion of the material from above (40 mg, 0.08 mmol) with 4-methoxyphenyl)boronic acid gave a residue that was hydrolyzed as described for **41**. Purification by RP-HPLC (method 1) afforded the title compound (12 mg, 30%) as a white solid. ^{1}H NMR (400 MHz, DMSO-d_6, 330 K) δ 1.11−1.39 (m, 5H), 1.60−1.79 (m, 5H), 1.80−1.90 (m, 2H), 1.91−2.12 (m, 2H), 2.50−2.61 (m, 2H), 2.76 (s, 6H), 2.90−3.10 (m, 1H), 3.35−3.50 (m, 1H), 3.87 (s, 3H), 3.93−4.15 (m, 1H), 4.37−4.46 (m, 1H), 4.90 (s, 2H), 7.08 (d, J = 8.3 Hz, 2H), 7.23 (d, J = 8.3 Hz, 2H), 7.64 (d, J = 8.4 Hz, 1H), 7.79 (d, J = 8.4 Hz, 1H), 7.92 (s, 1H), 9.64 (br s, 1H); MS (ES$^+$) m/z 518 (M + H)$^+$; RP-HPLC method 1, t_R = 7.0 min (>99%); method 2, t_R = 5.9 (>99%).

1-{6-Carboxy-3-cyclohexyl-2-(4-methoxyphenyl)-1H-indol-1-yl]acetyl}-N,N-diethylpiperidin-4-aminium Chloride (54). Step 1. Following the general procedure described for **55**, treatment of methyl 2-bromo-1-(2-$tert$-butoxy-2-oxoethyl)-3-cyclohexyl-1H-indole-6-carboxylate[15] (1.2 g, 2.67 mmol) with 4-methoxyphenyl)boronic acid gave a residue, which was purified by flash chromatography (5:95 EtOAc/petroleum ether) to give methyl 1-(2-$tert$-butoxy-2-oxoethyl)-3-cyclohexyl-2-(4-methoxyphenyl)-1H-indole-6-carboxylate (1.03 g, 81%). ^{1}H NMR (DMSO-d_6) δ 1.13−1.38 (m, 3H), 1.33 (s, 9H), 1.61−1.96 (m, 7H), 2.55−2.67 (m, 1H), 3.86 (s, 3H), 3.88 (s, 3H), 4.73 (s, 2H), 7.11 (d, J = 8.6 Hz, 2H), 7.27 (d, J = 8.6 Hz, 2H), 7.69 (dd, J = 8.4 Hz, J = 1.1 Hz, 1H), 7.86 (d, J = 8.4 Hz, 1H), 8.06 (d, J = 1.1 Hz, 1H).

Step 2. A solution of the compound from above (0.82 g, 1.71 mmol) in a 1:1 mixture of CH$_2$Cl$_2$ and TFA (20 mL) was stirred for 4 h and then concentrated in vacuo. The residue was triturated with Et$_2$O to afford [3-cyclohexyl-6-(methoxycarbonyl)-2-(4-methoxyphenyl)-1H-indol-1-yl]acetic acid (95%). ^{1}H NMR (DMSO-d_6) δ 1.13−1.36 (m, 3H), 1.62−1.95 (m, 7H), 2.56−2.67 (m, 1H), 3.86 (s, 3H), 3.89 (s, 3H), 4.74 (s, 2H), 7.12 (d, J = 8.6 Hz, 2H), 7.28 (d, J = 8.6 Hz, 2H), 7.69 (dd, J = 8.5 Hz, 1.2 Hz, 1H), 7.86 (d, J = 8.5 Hz, 1H), 8.02 (d, J = 1.2 Hz, 1H), 12.98 (br s, 1H).

Step 3. Following the general procedure described for **53**, treatment of the material from above (50 mg, 0.12 mmol) with N,N-diethylpiperidin-4-amine afforded a residue that was hydrolyzed as described for **41**. Purification by RP-HPLC (method 1) gave the title compound (26 mg, 33%) as a solid. ^{1}H NMR (DMSO-d_6) δ 1.12−1.49 (m, 5H), 1.29 (t, J = 7.1 Hz,

6H), 1.60−1.97 (m, 7H), 1.97−2.13 (m, 2H), 2.57−2.73 (m, 2H), 2.95−3.22 (m, 5H), 3.50−3.67 (m, 1H), 3.85 (s, 3H), 3.91−4.05 (m, 1H), 4.35−4.49 (m, 1H), 4.81−5.04 (m, 2H), 7.12 (d, J = 8.8 Hz, 2H), 7.25 (d, J = 8.8 Hz, 2H), 7.66 (d, J = 8.3 Hz, 1H), 7.83 (d, J = 8.3 Hz, 1H), 7.94 (s, 1H), 9.80 (br s, 1H), 12.52 (br s, 1H); MS (ES⁺) m/z 546 (M + H)⁺; RP-HPLC method 1, t_R = 7.1 min (>99%); method 2, t_R = 6.0 (>99%); HRMS calculated for $C_{33}H_{44}N_3O_4$ (M + H)⁺ 546.3326, found 546.3324.

1-{[6-Carboxy-2-(4-chlorophenyl)-3-cyclohexyl-1*H*-indol-1-yl]acetyl}-*N,N*-diethylpiperidin-4-aminium Chloride (55). Step 1: General Procedure for Suzuki Cross-Couplings. A solution of **60** (5.0 g, 15.9 mmol) in DME/EtOH (5:2) was treated with aqueous Na₂CO₃ (2 N, 8.5 equiv) and 4-chlorophenylboronic acid (2.8 g, 17.8 mmol) and then degassed. Pd(PPh₃)₄ (1.7 g, 1.48 mmol) was added, and the mixture was stirred at 80 °C for 6 h. The cooled solution was diluted with EtOAc and filtered through Celite. The filtrate was washed with brine, dried, and concentrated to afford a residue that was purified by flash chromatography (1:9 to 4:6 EtOAc/petroleum ether) to give methyl 2-(4-chlorophenyl)-3-cyclohexyl-1*H*-indole-6-carboxylate (4.40 g, 80%) as a white solid. ¹H NMR (400 MHz, DMSO-d_6) δ 1.22−1.45 (m, 3H), 1.67−1.85 (m, 5H), 1.90−2.06 (m, 2H), 2.78−2.90 (m, 1H), 3.86 (s, 3H), 7.55 (d, J = 8.3 Hz, 2H), 7.60 (d, J = 8.8 Hz, 1H), 7.62 (d, J = 8.3 Hz, 2H), 7.85 (d, J = 8.8 Hz, 1H), 7.99 (s, 1H), 11.56 (s, 1H); MS (ES⁺) m/z 368 (M + H)⁺.

Step 2. A solution of the material from above (3.2 g, 8.9 mmol) in DMF (100 mL) was cooled to 0 °C and treated with NaH (60% suspension in mineral oil, 0.30 g, 12.4 mmol). The mixture was stirred for 1 h and then treated with *tert*-butyl bromoacetate (3.50 g, 17.7 mmol). The resulting solution was stirred at 20 °C for 12 h and then diluted with EtOAc and aqueous HCl (1 N). The organic phase was separated, washed with brine, and dried. Removal of the solvent in vacuo afforded a residue that was purified by flash chromatography (1:99 to 1:9 EtOAc/petroleum ether) to give methyl 1-(2-*tert*-butoxy-2-oxoethyl)-2-(4-chlorophenyl)-3-cyclohexyl-1*H*-indole-6-carboxylate (4.0 g, 94%). ¹H NMR (DMSO-d_6) δ 1.11−1.34 (m, 3H), 1.29 (s, 9H), 1.60−1.94 (m, 7H), 2.52−2.63 (m, 1H), 3.87 (s, 3H), 4.76 (s, 2H), 7.36 (d, J = 8.4 Hz, 2H), 7.61 (d, J = 8.4 Hz, 2H), 7.69 (dd, J = 8.4 Hz, J = 1.0 Hz, 1H), 7.87 (d, J = 8.4 Hz, 1H), 8.09 (d, J = 1.0 Hz, 1H); ¹³C NMR (75 MHz, DMSO-d_6) δ 26.4, 27.4, 28.4, 33.6, 37.0, 47.0, 52.7, 82.5, 112.8, 120.3, 120.7, 120.9, 123.4, 129.6, 130.5, 130.6, 133.1, 134.7, 137.3, 139.6, 168.0, 168.8; MS (ES⁺) m/z 482 (M + H)⁺.

Step 3. A solution of the material from above (3.80 g, 7.8 mmol) in CH₂Cl₂ (20 mL) was cooled to 0 °C and treated with TFA (20 mL). The resulting solution was allowed to warm to room temperature and was then stirred for 6 h. The volatiles were removed under reduced pressure, and the residue was taken up in toluene. The mixture was concentrated in vacuo to afford [2-(4-chlorophenyl)-3-cyclohexyl-6-(methoxycarbonyl)-1*H*-indol-1-yl]acetic acid (3.30 g, 99%) as a pale-yellow solid. ¹H NMR (DMSO-d_6) δ 1.11−1.37 (m, 3H), 1.58−1.94 (m, 7H), 2.52−2.63 (m, 1H), 3.87 (s, 3H), 4.76 (s, 2H), 7.36 (d, J = 8.2 Hz, 2H), 7.62 (d, J = 8.2 Hz, 2H), 7.69 (d, J = 8.6 Hz, 1H), 7.87 (d, J = 8.6 Hz, 1H), 8.05 (s, 1H), 12.99 (br s,1H); ¹³C NMR (75 MHz, DMSO-d_6) δ 26.4, 27.4, 33.7, 37.0, 46.2, 52.7, 112.9, 120.1, 120.6, 120.9, 123.4, 129.7, 130.5, 130.6, 133.0, 134.7, 137.2, 139.7, 168.0, 171.1; MS (ES⁺) m/z 426 (M + H)⁺.

Step 4. Following the general amide coupling procedure described for **53**, treatment of the material from above (50 mg, 0.12 mmol) with *N,N*-diethylpiperidin-4-amine afforded a residue that was hydrolyzed as described for **41**. Purification by RP-HPLC (method 1) gave the title compound (54 mg, 70%) as a white solid. ¹H NMR (400 MHz, DMSO-d_6) δ 1.12−1.47 (m, 5H), 1.28 (t, J = 7.2 Hz, 6H), 1.57−1.79 (m, 5H), 1.79−1.93 (m, 2H), 1.95−2.06 (m, 2H), 2.51−2.59 (m, 1H), 2.59−2.71 (m, 1H), 2.98−3.20 (m, 5H), 3.50−3.63 (m, 1H), 3.91−4.02 (m, 1H), 4.32−4.44 (m, 1H), 4.85−5.06 (m, 2H), 7.34 (d, J = 8.5 Hz, 2H), 7.63 (d, J = 8.5 Hz, 2H), 7.66 (dd, J = 8.3 Hz, J = 1.3 Hz, 1H), 7.83 (d, J = 8.3 Hz, 1H), 7.97 (d, J = 1.3 Hz, 1H), 9.68 (br s, 1H), 12.56 (br s, 1H); ¹³C NMR (100 MHz, DMSO-d_6) δ 9.8, 25.5, 26.5, 32.8, 36.1, 39.9, 42.7, 43.9, 44.9,

58.0, 112.2, 118.7, 119.6, 119.7, 123.3, 128.6, 129.3, 130.1, 132.2, 133.6, 136.7, 138.5, 165.8, 168.2; MS (ES⁺) m/z 550 (M + H)⁺; RP-HPLC method 1, t_R = 7.5 min (>99%); method 2, t_R = 6.5 (>99%); HRMS calculated for $C_{32}H_{41}N_3O_3Cl$ (M + H)⁺ 550.2831, found 550.2819.

1-(1-{[6-Carboxy-3-cyclohexyl-2-(3-furyl)-1*H*-indol-1-yl]-acetyl}piperidin-4-yl)azetidinium Trifluoroacetate (56). Step 1. Following the general procedure described for **55**, treatment of **60** (0.50 g, 1.49 mmol) with 3-furylboronic acid afforded methyl 3-cyclohexyl-2-(3-furyl)-1*H*-indole-6-carboxylate (0.39 g, 81%). ¹H NMR (DMSO-d_6) δ 1.34−1.52 (m, 3H), 1.66−1.88 (m, 5H), 1.88−2.06 (m, 2H), 2.86−3.01 (m, 1H), 3.87 (s, 3H), 6.87 (d, J = 1.1 Hz, 1H), 7.59 (dd, J = 8.5 Hz, 1.4 Hz, 1H), 7.82 (d, J = 8.5 Hz, 1H), 7.86−7.90 (m, 1H), 7.98 (d, J = 1.1 Hz, 1H), 8.06 (s, 1H), 11.40 (s, 1H).

Step 2. A solution of the compound from above (0.39 g, 1.21 mmol) in DMF (20 mL) was cooled to 0 °C and treated with NaH (60% suspension in mineral oil, 41 mg, 1.69 mmol). The mixture was stirred for 0.5 h and then treated with *t*BuO₂-CCH₂Br (0.28 g, 1.45 mmol) and then warmed to 20 °C. The solution was stirred for 1 h, then diluted with EtOAc and aqueous HCl (1 N). The organic layer was separated, washed with brine, and dried. Removal of the solvent afforded a residue that was diluted with CH₂Cl₂ (4 mL) and then cooled to 0 °C. TFA (4 mL) was added, and the mixture was stirred for 4 h at 20 °C. The volatiles were removed and the residue was triturated with Et₂O to afford [3-cyclohexyl-2-(3-furyl)-6-(methoxycarbonyl)-1*H*-indol-1-yl]acetic acid (0.34 g, 76%). ¹H NMR (DMSO-d_6) δ 1.20−1.43 (m, 3H), 1.62−2.01 (m, 7H), 2.62−2.78 (m, 1H), 3.88 (s, 3H), 4.89 (s, 2H), 6.58 (d, J = 1. 1 Hz, 1H), 7.68 (dd, J = 8.5 Hz, 1.3 Hz, 1H), 7.80−7.94 (m, 3H), 8.06 (d, J = 1.1 Hz, 1H), 12.93 (br s, 1H).

Step 3. Following the general amide coupling procedure described for **53**, treatment of the compound from above (40 mg, 0.10 mmol) with 4-azetidin-1-ylpiperidine bis(trifluoroacetate) gave a residue that was hydrolyzed as described for **41**. Purification by RP-HPLC (method 4) afforded the title compound (30 mg, 48%) as a white solid. ¹H NMR (DMSO-d_6) δ 1.00−1.45 (m, 5H), 1.60−2.09 (m, 9H), 2.17−2.34 (m, 1H), 2.37−2.57 (m, 2H), 2.58−2.79 (m, 2H), 2.98−3.14 (m, 1H), 3.95−4.25 (m, 5H), 4.27−4.45 (m, 1H), 5.07 (s, 2H), 6.52 (s, 1H), 7.65 (d, J = 8.4 Hz, 1H), 7.79 (s, 1H), 7.82 (d, J = 8.4 Hz, 1H), 7.87 (s, 1H), 7.96 (s, 1H), 9.91 (br s, 1H), 12.31−12.88 (m, 1H); MS (ES⁺) m/z 490 (M + H)⁺; RP-HPLC method 1, t_R = 6.7 min (96%); method 2, t_R = 5.5 (95%); HRMS calculated for $C_{29}H_{36}N_3O_4$ (M + H)⁺ 490.2700, found 490.2687.

***N*-[(4-{[6-Carboxy-3-cyclohexyl-2-(4-methoxyphenyl)-1*H*-indol-1-yl]acetyl}morpholin-2-yl)methyl]-*N*-ethyl-ethanaminium Trifluoroacetate (57).** Following the general amide coupling procedure described for **53**, treatment of [3-cyclohexyl-6-(methoxycarbonyl)-2-(4-methoxyphenyl)-1*H*-indol-1-yl]acetic acid (70 mg, 0.17 mmol) with *N*-ethyl-*N*-(morpholin-2-ylmethyl)ethanamine gave a residue that was hydrolyzed as described for **41**. Purification by RP-HPLC (method 5) afforded the title compound (27 mg, 29%) as a white solid. ¹H NMR (400 MHz, DMSO-d_6) δ 1.10−1.35 (m, 9H), 1.60−1.78 (m, 5H), 1.80−1.92 (m, 2H), 2.53−2.63 (m, 1H), 2.72−2.95 (m, 1H), 3.10−3.21 (m, 6H), 3.22−3.35 (m, 1H), 3.38−3.52 (m, 1H), 3.60−3.95 (m, 6H), 4.09−4.27 (m, 1H), 4.78−5.05 (m, 2H), 7.02−7.14 (m, 2H), 7.24 (d, J = 8.3 Hz, 2H), 7.67 (d, J = 8.3 Hz, 1H), 7.81 (d, J = 8.3 Hz, 1H), 7.97 (s, 1H), 9.20 (br s, 1H); MS (ES⁺) m/z 562 (M + H)⁺; RP-HPLC method 1, t_R = 7.1 min (>99%); method 2, t_R = 6.1 (>99%); HRMS calculated for $C_{33}H_{44}N_3O_5$ (M + H)⁺ 562.3275, found 562.3290.

1-*tert*-Butyl 6-Methyl-3-cyclohexyl-2-(tributylstannyl)-1*H*-indole-1,6-dicarboxylate (61). Step 1. To a solution of **60** (0.50 g, 1.49 mmol) in CH₂Cl₂ (15 mL) were added 4-dimethylaminopyridine (0.19 g, 1.56 mmol) and di-*tert*-butyl dicarbonate (0.34 g, 1.56 mmol). The mixture was stirred at room temperature for 1.5 h and then diluted with CH₂Cl₂ and washed with aqueous HCl (1 N) and brine. The organic phase was dried and concentrated to give 1-*tert*-butyl 6-methyl-2-bromo-3-cyclohexyl-1*H*-indole-1,6-dicarboxylate (0.60 g, 93%) as a solid. ¹H NMR (DMSO-d_6) δ 1.33−1.50 (m, 3H), 1.67 (s,

9H), 1.70−2.10 (m, 7H), 2.90−3.09 (m, 1H), 3.89 (s, 3H), 7.83 (d, J = 8.2 Hz, 1H), 7.94 (d, J = 8.2 Hz, 1H), 8.69 (s, 1H).

Step 2. To a solution of 1-*tert*-butyl 6-methyl-2-bromo-3-cyclohexyl-1*H*-indole-1,6-dicarboxylate (1.00 g, 2.29 mmol) in THF (35 mL) was added ^{n}BuLi (1.86 mL, 2.98 mmol 1.6 N in hexane) dropwise at −78 °C. After 15 min tributyl(chloro)-stannane (1.12 g, 3.43 mmol) was added dropwise and the mixture was allowed to warm to room temperature. Then the reaction was quenched with H_2O and EtOAc. The organic phase was separated and then washed with brine and dried. Removal of the solvent afforded a residue that was purified by flash chromatography (2:98 EtOAc/petroleum ether) to afford the title compound (0.92 g, 64%) as a solid. ^{1}H NMR (CDCl$_3$) δ 0.88 (t, J = 7.1 Hz, 9H), 0.94−1.19 (m, 6H), 1.20−1.46 (m, 9H), 1.48−1.62 (m, 9H), 1.68 (s, 9H), 1.70−2.12 (m, 4H), 2.78−2.95 (m, 1H), 3.94 (s, 3H), 7.76 (d, J = 8.4 Hz, 1H), 7.83 (d, J = 8.4 Hz, 1H), 8.74 (s, 1H).

Supporting Information Available: Mass spectrometry data and RP-HPLC purities for compounds **2**−**8** and **10**−**37** and experimental procedures and spectral data for compounds **44** and **47**−**52**. This material is available free of charge via the Internet at http://pubs.acs.org.

References

(1) Choo, Q.-L.; Kuo, G.; Weiner, A. J.; Overby, L. R.; Bradley, D. W.; Houghton, M. Isolation of a cDNA Clone Derived from a Blood-borne Non-A, Non-B Viral Hepatitis Genome. *Science* **1989**, *244*, 359−362.

(2) Sarbah, S. A.; Younossi, Z. M. Hepatitis C: An Update on the Silent Epidemic. *J. Clin. Gastroenterol.* **2000**, *30*, 125−143.

(3) NIH Consensus Statements. *Management of Hepatitis C*; National Institutes of Health: Bethesda, MD, 2002; Vol. 19, Issue 1.

(4) Dymock, B. W. Emerging Therapies for Hepatitis C Virus Infection. *Emerging Drugs* **2001**, *6*, 13−42.

(5) Lohmann, V.; Korner, F.; Koch, J.; Henan, U.; Theilmann, L.; Bartenschlager, R. Replication of Subgenomic Hepatitis C Virus RNA's in a Hepatoma Cell Line. *Science* **1999**, *285*, 110−113.

(6) Tan, S.-L.; Victor, F.; Chen, S.-H. HCV Protease Inhibitors as Potential Therapeutic Agents for the Treatment of HCV Infection. *Front. Biotechnol. Pharm.* **2004**, *4* 123−146.

(7) Hinrichsen, H.; Benhamou, Y.; Wedemeyer, H.; Reiser, M.; Sentjens, R. E.; Calleja, J. L.; Forns, X.; Erhardt, A.; Crönlein, J.; Chaves, R.; Yong, C.-L.; Nehmiz, G.; Steinmann, G. G. Short-Term Antiviral Efficacy of BILN 2061, a HCV Serine Protease Inhibitor, in Hepatitis C Genotype 1 Patients. *Gastroenterology* **2004**, *127*, 1347−1355.

(8) Beaulieu, P. L.; Tsantrizos, Y. S. Inhibitors of the HCV NS5B Polymerase: New Hope for the Treatment of Hepatitis C Infections. *Curr. Opin. Invest. Drugs* **2004**, *5*, 838−850.

(9) Lesburg, C. A.; Cable, M. B.; Ferrari, E.; Hong, Z.; Mannarino, A. F.; Weber, P. C. Crystal Structure of the RNA-Dependent RNA Polymerase from Hepatitis C Virus Reveals a Fully Encircled Active Site. *Nat. Struct. Biol.* **1999**, *6*, 937−943.

(10) LaPlante, S.; Jakalian, A.; Aubry, N.; Bousquet, Y.; Ferland, J.-M.; Gillard, J.; Lefebvre, S.; Poirier, M.; Tsantrizos, Y. S.; Kukolj, G.; Beaulieu, P. L. Drug Design: Binding Mode Determination of Benzimidazole Inhibitors of the Hepatitis C Virus RNA Polymerase by a Structure and Dynamics Strategy. *Angew. Chem., Int. Ed.* **2004**, *43*, 4306−4311.

(11) Carroll, S. S.; Tomassini, J. E.; Bosserman, M.; Getty, K.; Stahlhut, M. W.; Eldrup, A. B.; Bhat, B.; Hall, D.; Simcoe, A. L.; LaFemina, R.; Rutkowski, C. A.; Bohdan, W.; Yang, Z.; Migliaccio, G.; De Francesco, R.; Kuo, L. C.; MacCoss, M.; Olsen, D. B. Inhibition of Hepatitis C Virus RNA Replication by 2′-Modified Nucleoside Analogs. *J. Biol. Chem.* **2003**, *278*, 11979−11984.

(12) Dhanak, D.; Duffy, K. J.; Johnston, V. K.; Lin-Goerke, J.; Darcy, M.; Shaw, A. N.; Gu, B.; Silverman, C.; Gates, A. T.; Nonnemacher, M. R.; Earnshaw, D. L.; Casper, D. J.; Kaura, A.; Baker, A.; Greenwood, C.; Gutshall, L. L.; Maley, D.; DelVecchio, A.; Macarron, R.; Hofmann, G. A.; Alnoah, Z.; Cheng, H.-Y.; Chan, G.; Khandekar, S.; Keenan, R. M.; Sarisky, R. T. Identification and Biological Characterization of Heterocyclic Inhibitors of the Hepatitis C Virus RNA-Dependent RNA Polymerase. *J. Biol. Chem.* **2002**, *277*, 38322−38327.

(13) (a) Chan, L.; Das, S. K.; Reddy, T. J.; Poisson, C.; Proulx, M.; Pereira, O.; Courchesne, M.; Roy, C.; Wang, W.; Siddiqui, A.; Yannopoulos, C. G.; Nguyen-Ba, N.; Labrecque, D.; Bethell, R.; Hamel, M.; Courtemanche-Asselin, P.; L'Heureux, L.; David, M.; Nicolas, O.; Brunette, S.; Bilimoria, D.; Bedard, J. Discovery of Thiophene-2-carboxylic Acids as Potent Inhibitors of HCV NS5B Polymerase and HCV Subgenomic RNA Replication. Part 1: Sulfonamides. *Bioorg. Med. Chem. Lett.* **2004**, *14*, 793−796. (b) Chan, L.; Pereira, O.; Reddy, T. J.; Das, S. K.; Poisson, C.; Courchesne, M.; Proulx, M.; Siddiqui, A.; Yannopoulos, C. G.; Nguyen-Ba, N.; Roy, C.; Nasturica, D.; Moinet, C.; Bethell, R.; Hamel, M.; L'Heureux, L.; David, M.; Nicolas, O.; Courtemanche-Asselin, P.; Brunette, S.; Bilimoria, D.; Bedard, J. Discovery of Thiophene-2-carboxylic Acids as Potent Inhibitors of HCV NS5B Polymerase and HCV Subgenomic RNA Replication. Part 2: Tertiary Amides. *Bioorg. Med. Chem. Lett.* **2004**, *14*, 797−800.

(14) Beaulieu, P. L.; Bousquet, Y.; Gauthier, J.; Gillard, J.; Marquis, M.; McKercher, G.; Pellerin, C.; Valois, S.; Kukolj, G. Non-Nucleoside Benzimidazole-Based Allosteric Inhibitors of the Hepatitis C Virus NS5B Polymerase: Inhibition of Subgenomic Hepatitis C Virus RNA Replicons in Huh-7 Cells. *J. Med. Chem.* **2004**, *47*, 6884−6892.

(15) Harper, S.; Pacini, B.; Avolio, S.; Di Filippo, M.; Migliaccio, G.; Laufer, R.; De Francesco, R.; Rowley, M.; Narjes, F. Development and Preliminary Optimization of Indole-*N*-Acetamide Inhibitors of Hepatitis C Virus NS5B Polymerase. *J. Med. Chem.* **2005**, *48*, 1314−1317.

(16) (a) Tomei, L.; Altamura, S.; Bartholomew, L.; Biroccio, A.; Ceccacci, A.; Pacini, L.; Narjes, F.; Gennari, N.; Bisbocci, M.; Incitti, I.; Orsatti, L.; Harper, S.; Stansfield, I.; Rowley, M.; De Francesco, R.; Migliaccio, G. Mechanism of Action and Antiviral Activity of Benzimidazole-Based Allosteric Inhibitors of the Hepatitis C Virus RNA-Dependent RNA Polymerase. *J. Virol.* **2003**, *77*, 13225−13231. (b) McKercher, G.; Beaulieu, P. L.; Lamarre, D.; LaPlante, S.; Lefebvre, S.; Pellerin, C.; Thauvette, L.; Kukolj, G. Specific Inhibitors of HCV Polymerase Identified Using an NS5B with Lower Affinity for Template/Primer Substrate. *Nucleic Acids Res.* **2004**, *32*, 422−431.

(17) (a) El-Sankary, W.; Gibson, G. G.; Ayrton, A.; Plant, N. Use of a Reporter Gene Assay To Predict and Rank the Potency and Efficacy of CYP3A4 Inducers. *Drug Metab. Dispos.* **2001**, *29* 1499−1504. (b) Ogg, M. S.; Williams, J. M.; Tarbit, M.; Goldfarb, P. S.; Gray, T. J.; Gibson, G. G. A Human Reporter Gene Assay To Assess the Molecular Mechanisms of Xenobiotic-Dependent Induction of the Human CYP3A4 Gene in-Vitro. *Xenobiotica* **1999**, *29*, 269−279.

(18) Full details on the binding mode and mechanism of action of **1** when bound to the NS5B enzyme will be published elsewhere. DiMarco, S.; Volpari, C.; Tomei, L.; Altamura, S.; Harper, S.; Narjes, F.; Koch, U.; Rowley, M.; De Francesco, R.; Migliaccio, G.; Carfi, A. Interdomain Communication in NS5B HCV Polymerase Abolished by Small-Molecule Inhibitors Bound to a Novel Allosteric Site. Manuscript submitted.

(19) Rodgers, J. D.; Lam, P. Y. S.; Johnson, B. L.; Wang, H.; Ko, S. S.; Seitz, S. P.; Trainor, G. L.; Anderson, P. S.; Klabe, R. M.; Bacheler, L. T.; Cordova, B.; Garber, S.; Reid, C.; Wright, M. R.; Chang, C.-H.; Erickson-Viitanen, S. Design and Selection of DMP 850 and DMP 851: The Next Generation of Cyclic Urea HIV Protease Inhibitors. *Chem. Biol.* **1998**, *5*, 597−608 and references therein.

(20) Goodwin, B.; Redinbo, M. R.; Kliewer, S. A. Regulation of CYP3A Gene Transcription by the Pregnane X Receptor. *Ann. Rev. Pharmacol. Toxicol.* **2002**, *42* 1−23.

(21) MDS Pharma Services Taiwan Ltd., Pharmacology Laboratories, 158 Li-The Road, Peitou, Taipei, Taiwan 112, R.O.C.

(22) Lamarre, D.; Anderson, P. C.; Bailey, M.; Beaulieu, P.; Bolger, G.; Bonneau, P.; Boes, M.; Cameron, D. R.; Cartier, M.; Cordingley, M. G.; Faucher, A.-M.; Goudreau, N.; Kawai, S. H.; Kukolj, G.; Lagace, L.; LaPlante, S. R.; Narjes, H.; Poupart, M.-A.; Rancourt, J.; Sentjens, R. E.; St. George, R.; Simoneau, B.; Steinmann, G.; Thibeault, D.; Tsantrizos, Y. S.; Weldon, S. M.; Yong, C.-L.; Llinas-Brunet, M. An NS3 Protease Inhibitor with Antiviral Effects in Humans Infected with Hepatitis C Virus. *Nature* **2003**, *426*, 186−189.